Asian Journal of Information Technology 15 (23): 4861-4874, 2016
ISSN: 1682-3915

Energy Forecasting for Grid Connected Solar PV System Based on Weather Classification

Ashwin Kumar Sahoo
Department of EEE, SSN College of Engineering, OMR, Kalavakkam,
603110 Chennai, Tamil Nadu, India

Abstract: In recent years focus has been on environmental pollution issue resulting from consumption of fossil fuels, e.g., coal and oil. Thus introduction of an alternative energy source such as solar Photo Voltaic (PV) energy is gaining momentum. Short-term photovoltaic power generation forecasting is an important task in renewable energy power system planning and operation. Based on seasonal weather classification, the Back Propagation (BP) Artificial Neural Network (ANN) approach is utilized to forecast the next 24 h PV power outputs, using weather database which include global irradiance, temperature, wind speed and humidity data of Chennai city (South-East coast of India) using a data acquisition system. The estimated results of the proposed PV power forecasting model coincide well with measurement data for a 10 kW roof top grid connected PV system. The future DC and AC power outputs are predicted for any given day. The proposed approach achieves better prediction accuracy for hot and humid climatic region.

Key words: Roof top grid connected PV system, solar PV forecasting, artificial neural network, back propagation algorithm, weather classification

INTRODUCTION

The economic survey, tabled in the indian parliament notes that sweeping changes have been made in the power sector in the last 2 year. Year 2014-15 witnessed the highest ever increase in generation capacity of 26.5 GW compared to the average annual addition of around 19 GW over the past 5 years. Capacity enhancements have brought down the peak electricity deficit to its lowest ever level of 2.4 %. The survey states that renewable energy targets have been revised from 32-175 GW to give a policy push to the renewable sector and sustainable development. Among Renewable Energy Sources (RES), solar energy has the greatest energy potential and PV arrays permit to produce electric power directly from sunlight; furthermore, during the operational phase, the energy production occurs without fossil-fuel consumption or noise and not posing health and environmental hazards. These features will make the PV devices one of the most important among the technologies based on the exploitation of RES . Again Grid parity for solar generation is on its way to becoming a reality with auctions under the national solar mission resulting in all time low tariff of around Rs. 5 kW h^{-1}.

Forecast information is essential for an efficient use, the management of the electricity grid and for solar energy trading. Some studies have been carried out on this (Cao *et al*., 2009) but in general, there is little information on the topic. The most severe disturbance caused by the connection of a large amount of PV generation to the grid would be encountered when a band of cloud sweeps over an area with a large concentration of PV generators (Yang *et al*., 2014). This could result in a fairly large and sudden variation in the PV output. The condition would be aggravated if this change in irradiance occurred during a rapid increase in load. For these reasons, it is clear that the availability of reliable predictive tools is very important for the dissemination of PV technologies, to optimize the performance of PV systems in the planning and operational phase and finally to correctly assess the economic return. Solar power forecasting involves knowledge of the Sun's path, the atmosphere's condition on the incoming radiation, the scattering processes and the characteristics of a solar energy plant which utilizes the Sun's energy to create solar power (Yona *et al*., 2008).

Location dependence: Solar resources are based in specific locations and, unlike coal, gas, oil or uranium, cannot be transported to a generation site that is grid optimal. Generation must be co-located with the resource itself . The need for a one-day ahead forecasting of the energy production on an hourly basis, by means of soft computing techniques starting from weather forecast

provided by meteorological service, can play a fundamental role and becomes extremely useful for optimal management of the energy system (Tanaka *et al*., 2011).

MATERIALS AND METHODS

PV forecasting and method followed: Since, there are various factors affecting PV power generation, it is difficult to express the power outputs with a fixed mathematical function. Much research has been devoted to the forecasting of PV power generation (Capizzi *et al*., 2012). These techniques can roughly be categorized into two types: the indirect forecasting methods and direct forecasting methods. For the indirect methods, solar irradiance is predicted based on historical solar irradiance and weather data and then is converted to PV power output. The techniques used include fuzzy logic method, wavelet analysis, Artificial Neural Network (ANN) and hybrid ANN-based methods (Oudjana *et al*., 2012). The direct methods predict PV power output according to their historical data and associated weather information. The techniques used consist of Support Vector Regression (SVR), ANN and hybrid ANN methods (Ran and Guangmin, 2008; Shi *et al*., 2012).

These methods as mentioned above are useful for PV power output forecasting. However, the fuzzy logic-based method can not learn directly from historical data (Yu and Chang, 2011). The limitations of wavelet analysis are the complex model structure and the high computational cost required. Moreover, ANN-based methods can be used for all the classification and forecasting problems but require the user to specify various parameters of the model, especially those related to the network topology. The unpredictable and nonlinear relationship between power outputs and multiple meteorological factors also implies that different weather types will lead to significant variation in PV power outputs.

Chennai has a hot and humid climate. The city lies on the thermal equator and is also on the coast of bay of Bengal which prevents extreme variation in seasonal temperature. The hottest part of the year is late April to early June, with maximum temperatures around 35-40°C (95-104°F). The coolest part of the year is January, with minimum temperatures around 19-25 C (66-77°F). The average annual rainfall is about 140 cm (55 in). The city gets most of its seasonal rainfall from the North-East monsoon winds, from mid-October to mid-december. Prevailing winds in Chennai are usually South Westerly between April and October and North-Easterly during the rest of the year. Therefore, the outputs should be modeled with respect to different meteorological parameters and predicted under different weather types separately, namely winter, summer and rainy (cloudy) season.

Modelling of neural network: Artificial Neural Network (ANN) is based on the idea of human neurons and uses a large number of artificial neurons to imitate the capabilities of neural network in the living creatures (Wang *et al*., 2011). In recent years, Back Propagation (BP) neural network is one of the most widely used ANNs because of its simplicity for implementation. Typical BP network employs a multilayered feed-forward topology and the basic structure of a three-layer BP network has been shown in Fig. 1. The input variable of BP network is X = [x EMBED Equation.3 X = [x EMBED Equation. The 3, ..., X = [x EMBED Equation. The 3 hidden layer unit is $L = [L_1, L_2, \ldots\ldots L_m]^T$, output variable is $Y = [y_1, y_2, \ldots\ldots y_1]^T$. The weight connected between input layer units and hidden layer unit h_j is $V = [v_1, v_2, \ldots\ldots v_n]^T$. The weight connected between hidden layer units and output unit y_k is $W = [w_1, w_2, \ldots\ldots w_n]^T$. For output layer:

$$y_k, f(n_k) k = 1, 2, \ldots\ldots 1 \quad (1)$$

$$n_k = \sum_{j=1}^{m} w_{jk} h_k + b \quad k =, 1\ 2, \ldots\ldots 1 \quad (2)$$

For hidden layer:

$$h_j = f(n_j), j = 1, 2, \ldots\ldots m \quad (3)$$

$$n_j = \sum_{i=1}^{n} v_{ij} + h_j + b \quad j = 1, 2, \ldots\ldots m \quad (4)$$

The transfer function of the neurons is chosen as the most widely used sigmoid function, to test the proposed PV power forecasting model which can be expressed as follows:

$$f(x) \frac{1}{1+e^{-x}} \quad (5)$$

In the proposed 3 layer ANN structure, there are seven input variables and two output variables as shown in Fig.1. Usually, there is no general method to decide the most suitable number of hidden layer neurons. Empirical formula of m = (l+ n)/2 has been adopted initially and then

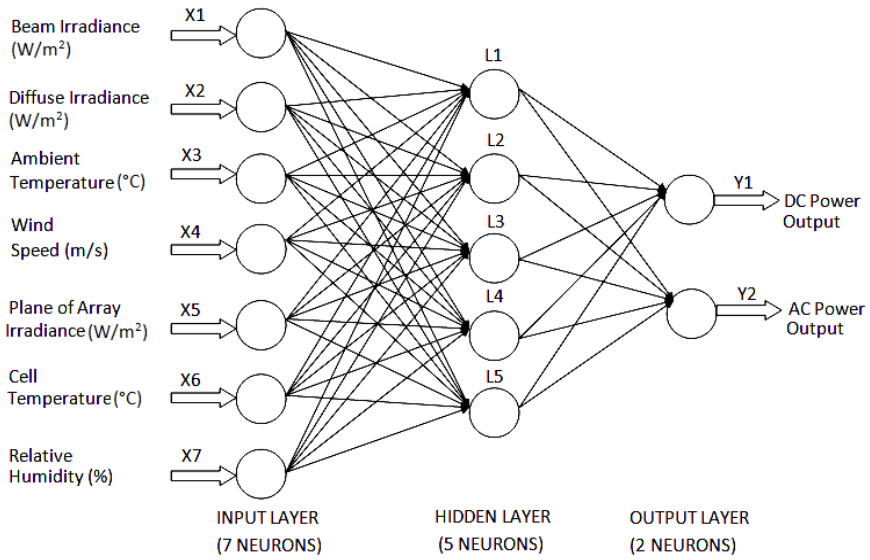

Fig. 1: Neural network structure (3 layer)

Table1: System specification

Specifications	Type
Location	Chennai coast
Latitude (degree N)	13.05
Longitude (degree E)	80.25
Elevation (m)	17
DC system size (kW)	10
Module type	Standard
Array type	Fixed (open rack)
Array tilt (°)	20
Array azimuth (°)	180
System losses (%)	14
Invert efficiency (%)	96
DC to AC size ratio	1.1

simple "trial-and-error" method was then used to find a suitable number m with balanced precision and computational burden. Finally, it is chosen to be five neurons with optimal mapping in this study, after repeatedly testing of the forecasting performance of the neural network.

Since, the value of sigmoid function is in the range of 0-1, the training data should be normalized before being applied to the BP neural network. The normalization of meteorological parameters and PV output power is written as:

$$\bar{x}_i \frac{x_i - x_{min}}{x_{max} - x_{min}} \quad (5)$$

Where:

x_I = The ith component in the original input data vector

x_{min} and x_{mi} = The minimum and maximum values of the input data vector separately

The gradient decent method is applied in the training process which yields a faster convergence rate (Liu *et al*., 2015).

Data collection, training and testing: Among ANN-related methods, Back Propagation (BP) neural network has been more widely used because of its excellent nonlinear characteristics. BP neural network has the advantages of complex nonlinear systems simulation ability, good approximation performance, strong learning ability and large fault data tolerance. The proposed day ahead forecasting comprises the following:

- Data collection
- Training and testing and
- Prediction

The hourly average data of the weather parameters such as beam irradiance, diffuse irradiance, ambient temperature, cell temperature, wind speed, percentage humidity, plane of array irradiance, dc array output and ac array output power are collected. All the collected time series data (365 days) were divided in two sets: training and testing data sets. The training data set included 70% of the time series data, the testing and validation data set 30%. These forecast values are compared with the actual values recorded at site. Figure 2 shows the basic flow chart to design an artificial neural network model in steps. The tested data are acquired from the PV system located in the SSN Institution campus, Chennai coast india. The rated power of the PV system is 10KW. The site specifications is given in Table 1. The entire data

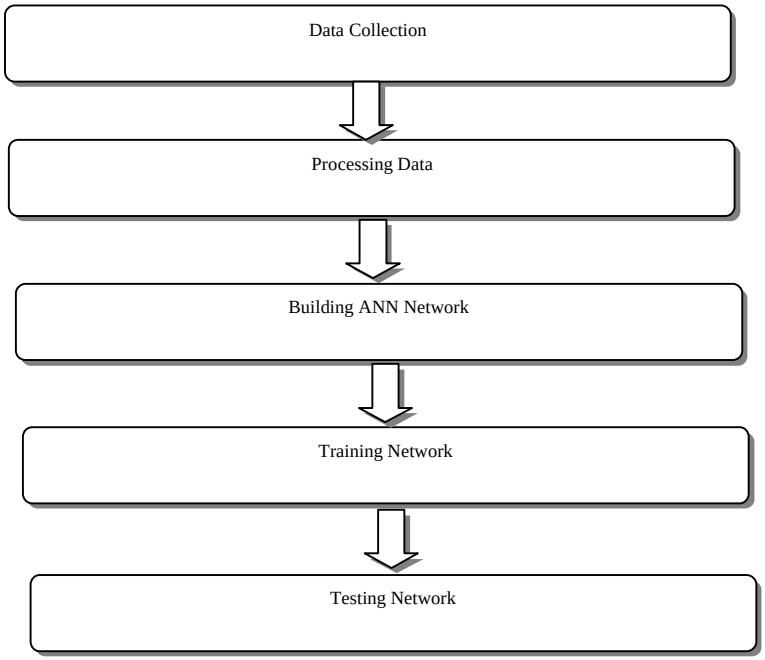

Fig. 2: Basic flow for designing artificial neural network model

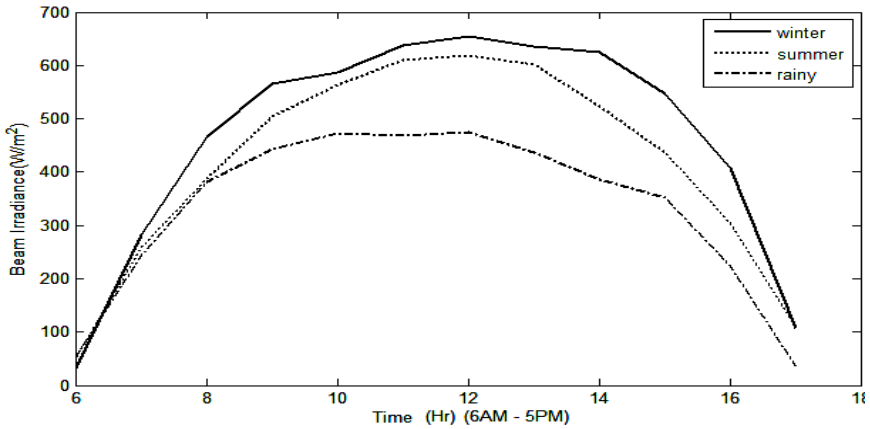

Fig. 3: Beam irradiance vs time

comprises of 12 months of 365 day, parameter variations from 6.00 AM-5.00 PM.

Before prediction being performed, historical data including meteorological parameters and hourly power outputs are classified into several categories according to weather types. The entire data was divided into three different seasons AS felt in Chennai coast. Each season comprising of months as follows:

- Winter season (December, January, February)
- Summer season (March, April, May, June, July, August)
- Rainy/cloudy season (September, October, November)

After dividing, the average values for each parameter was taken for the three seasons. A sample of the collected data is shown below Table 2.

Seasonal variations of input parameters: Due to the absence of suspended particles in the atmosphere the beam irradiance is more in winter as shown in Fig. 3. Whereas it is moderate in summer and less in rainy season.

Since, the direct irradiance gets scattered back to the atmosphere due to more suspended particles in summer, the diffuse irradiance is more in summer, moderate in rainy and less in winter which is shown in Fig. 4. Ambient temperature is nothing but the surrounding temperature

Table 2: Everage data for the seasons

Season 1 winter hour	6:00 AM	7:00 AM	8:00 AM	9:00 AM	10:00 AM	11:00 AM	12:00 AM	1:00 AM	2:00 AM	3:00 AM	4:00 AM	5:00 AM
Beam Irradiance (W m^{-2})	32.81	281.55	466.98	566.44	587.06	636.85	654.8	635.06	624.45	545.93	407.04	107.15
Diffuse irradiance (W m^{-2})	1.53	88.04	155.61	203.39	243.39	249.34	250.37	235.42	201.61	172.04	120.87	42.07
Ambient temperature (C)	23.76	24.7	26.47	27.93	29.01	29.66	29.81	29.52	28.81	27.65	26.13	24.6
Wind speed (m sec^{-1})	1.7	1.72	1.89	2.01	2.11	2.2	2.28	2.35	2.45	2.54	2.58	2.67
Relative humidity (%)	99	94	83	76	65	58	64	59	59	49	49	55
Plane of array irradiance (W m^{-2})	0	159.03	331.98	538.51	701.9	834.57	903.32	885.14	805.18	641.02	408.61	99.24
Cell temperature (C)	23.76	27.49	34.57	41.79	47.35	51.41	53.36	52.48	49.68	44.28	36.54	26.62
DC array output (W)	0	1212.07	2551.49	4157.58	5350.23	6250.56	6711.67	6553.5	6089.05	4997.38	3265.34	796.56
AC system output (W)	0	1132.02	2438.75	3997.31	5148.42	6013.97	6456.79	6303.97	5857.89	4807.31	3131.54	727.25
Season 2 summer hour												
Beam irradiance (W m^{-2})	52.83	258.83	388.48	504.47	563.21	611.01	617.96	601.07	523.99	437.21	303.19	109.71
Diffuse irradiance (W m^{-2})	61.33	154.44	212.48	247.03	270.29	278.7	283.14	264.45	254.54	216.3	169.04	85.08
Ambient temperature (C)	27.82	29.46	31.53	33.33	34.71	35.47	35.71	35.48	34.84	33.91	32.74	31.17
Wind speed (m sec^{-1})	2.67	2.59	2.54	2.44	2.34	2.226	2.22	2.24	2.3	2.39	2.59	2.84
Relative humidity (%)	66	66	63	58	52	47	44	41	40	38	36	40
Plane of array irradiance (W m^{-2})	52.76	134.47	310.2	493.21	650.93	774.15	818.67	802.12	694.45	533.36	334.73	119.98
Cell temperature (C)	27.59	31.62	38.38	45.3	51.2	55.52	57.2	56.63	53.29	47.98	41.24	23.96
DC array output (W)	478.54	1035.98	2328.29	3725.81	4848.41	5660.17	5935	5834.97	5136.29	4042.01	2601	946.73
AC system output (W)	422.44	959.83	2221.28	3578.76	4664.36	5446.62	5910.76	5614.43	4941.09	3883.78	2486.2	872.38
Season 1 rainy												
Beam irradiance (W m^{-2})	53.57	244.6	380.87	443.35	471.78	467.53	475.48	435.74	386.84	351.76	224.04	35.95
Diffuse irradiance (W m^{-2})	38.66	120.85	134.85	233.55	253.11	268.07	275.03	262.38	231.67	182.24	110.88	24.83
Ambient temperature (C)	25.38	26.32	27.82	29	29.8	30.2	30.3	30.13	29.72	29.1	28.17	27.17
Wind speed (m sec^{-1})	2.18	2.09	2.18	2.25	2.27	2.26	2.27	2.28	2.29	2.27	2.24	2.29
Relative humidity (%)	94	84	84	79	74	70	63	56	49	49	49	59
Plane of array irradiance (W m^{-2})	0	172.1	345.96	514.52	636.85	708.7	754.45	700.75	592.18	465.96	250.01	38.47
Cell temperature (C)	25.38	29.4	35.94	41.82	46.09	48.63	50.09	48.76	45.6	41.54	34.72	27.45
DC array output (W)	0	1323.56	2691.83	3998.38	4862.55	5333.78	5640.42	5235.69	4422.29	3638.02	2001.06	310.24
AC system output (W)	0	1243.22	2574.8	3841.72	4675.09	5128.04	5423.54	5065.27	4345.24	3491.03	1900.49	259.98

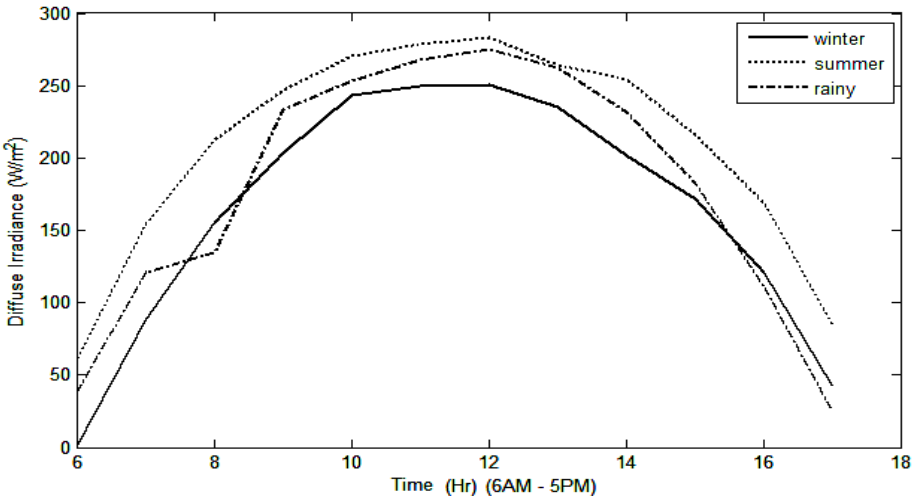

Fig. 4: Diffuse irradiance vs time

of the system. The seasonal variation is shown in Fig. 5. It has a positive correlation with the efficiency of the PV system. Wind speed is caused by air moving from high pressure area to low pressure area. During winter the wind

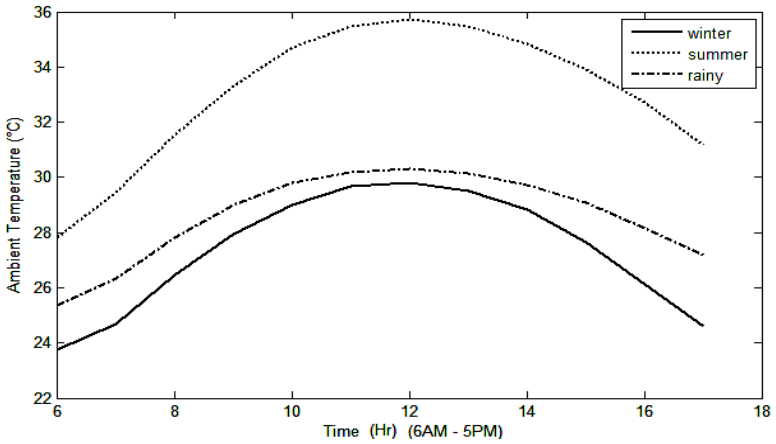

Fig.5: Ambient temperature vs time

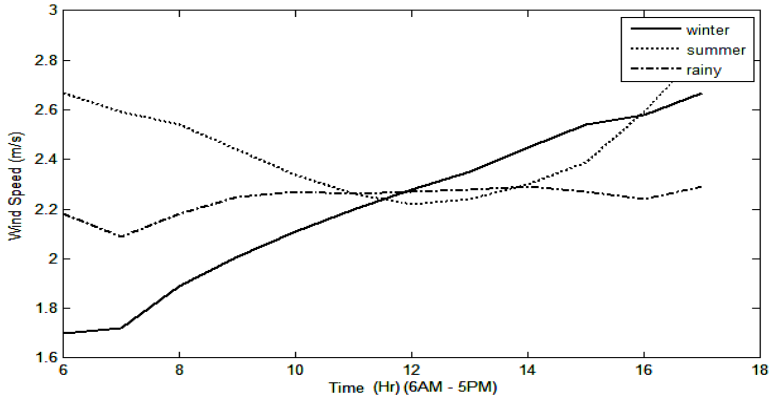

Fig.6 Wind speed vs time

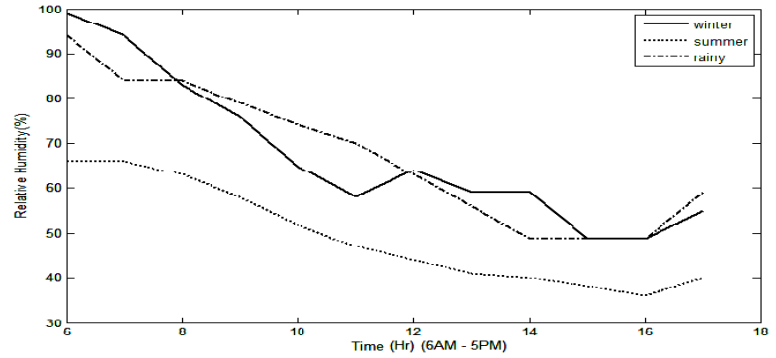

Fig.7: Relative humidity vs time

is very less in the morning hours and it gradually rises as the time extends. There is no drastic change in wind speed in summer and rainy seasons as shown in Fig. 6. Since Chennai is a tropical city, even though the climate is very hot in summer, there occurred no rainfall during summer and hence from Fig. 7, it is clear that the relative humidity is less in summer. The energy production efficiency of solar panel will be high at minimum humidity. The plane of array irradiance is the total amount of radiation that falls of the array of panels taking both the beam and the

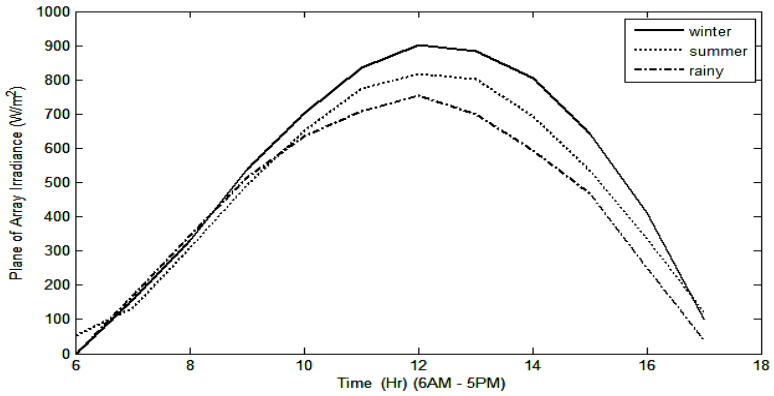

Fig. 8: Plane of array irradiance vs time

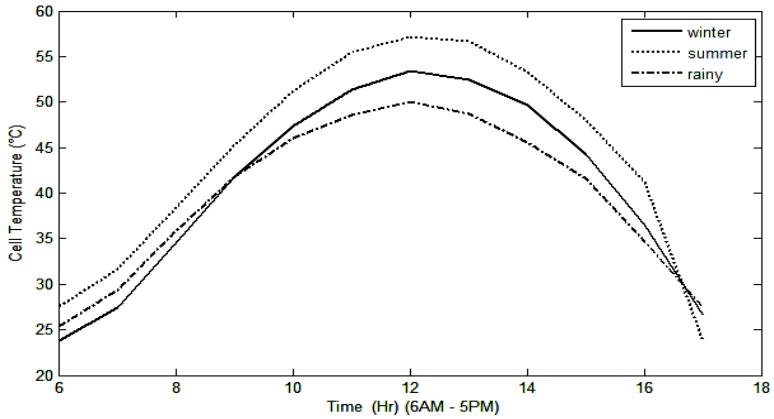

Fig. 9: Cell temperature vs time

diffuse irradiances into consideration. From Fig. 8, it is more in winter, moderate in summer and less in rain. The energy production efficiency of solar cell decreases when it reaches hot temperature. Figure 9 shows that the cell temperature is high in summer. The average data of three seasons was normalized using Eq. 6.

RESULTS AND DISCUSION

Simulation results and analysis: Data were recorded through weather forecast every day and stored inside each PV power plant. Then, the historical data with the same weather type as that of the objective day are chosen as the training samples of the BP neural network. With the well-trained BP neural network, PV power outputs can be predicted by importing the historical output power of selected days and the meteorological parameters of the objective day. Finally, the predicted output power of the PV system will be exported and compared with the measurement data, so as to verify the validity of the proposed forecasting model. The performances of the PV power forecasting model on winter, summer and cloudy days are shown as follows:

Winter season: It is clear from the performance plot (Fig. 10) that the Mean Square Error (MSE) value obtained is nearer to the calculated value. The regression plots obtained after training shows how far the data are within the fit at each phase (Fig.11).

From the regression plot (Fig. 12) obtained from testing the network shows how far the data lies within the fit after testing process.

The forecasted values (trained output) of hourly PV power and measured power (actual output) for the winter season are tabulated in Table 3 with their errors. The DC and AC actual and trained output are depicted in Fig. 13 and 14, respectively.

Summer season: Similarly, for summer season, it is clear from the performance plot (Fig. 15) that the Mean Square Error (MSE) value obtained is nearer to the calculated value. The regression plots obtained after training shows

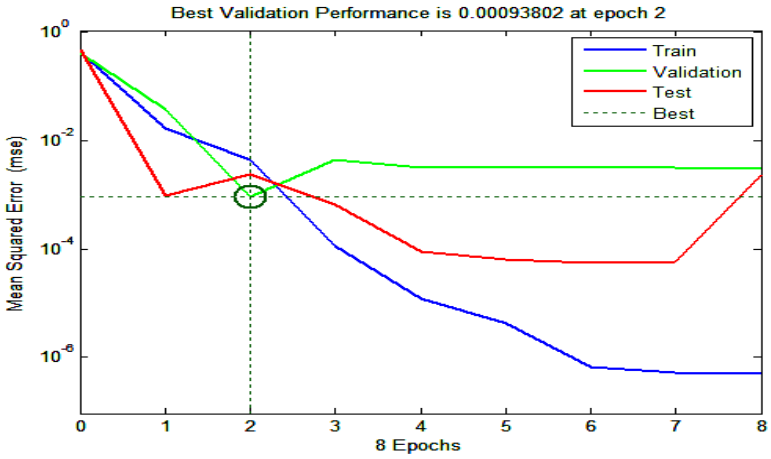

Fig. 10: Performance plot-Winter

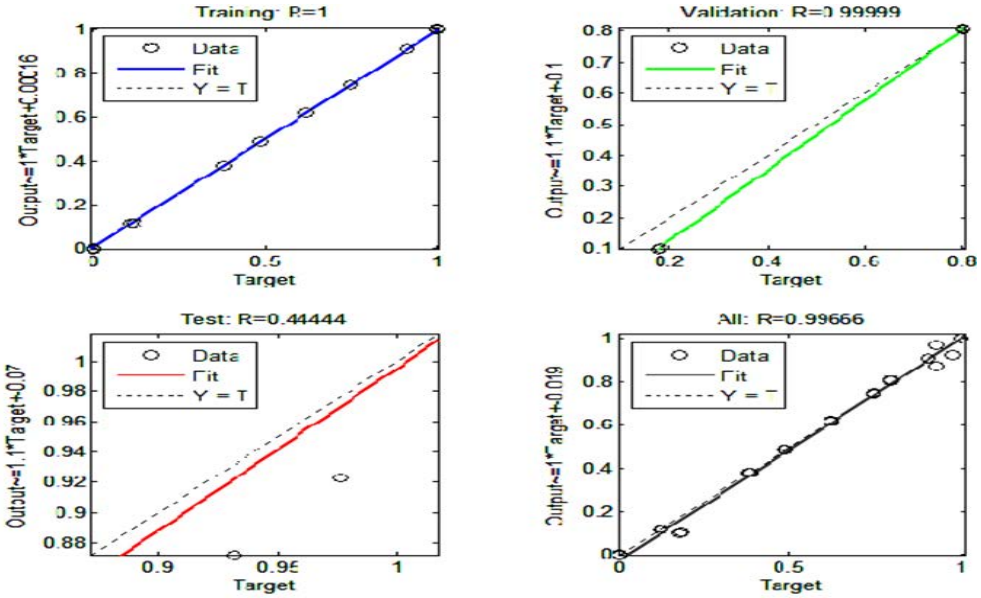

Fig. 11: Training regression plot-Winter

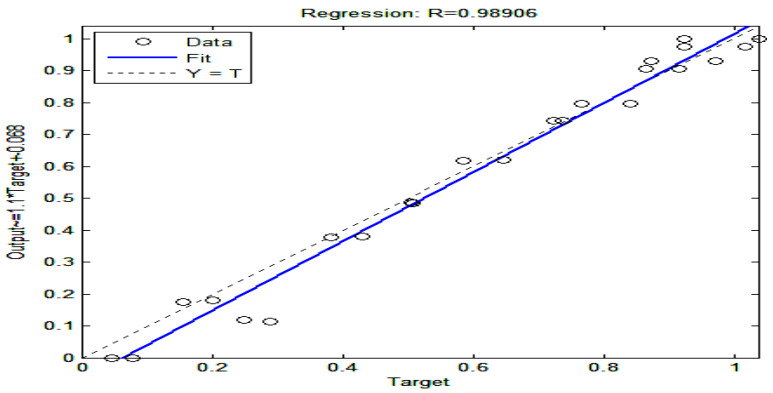

Fig. 12: Testing regression plot-Winter

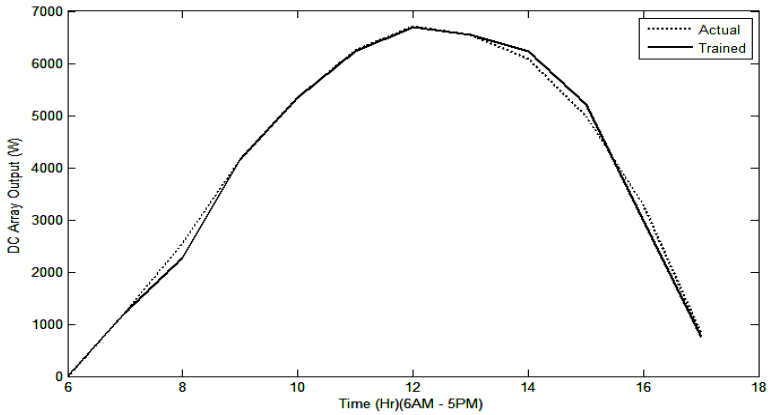

Fig. 13: DC actual and trained output vs time-Winter

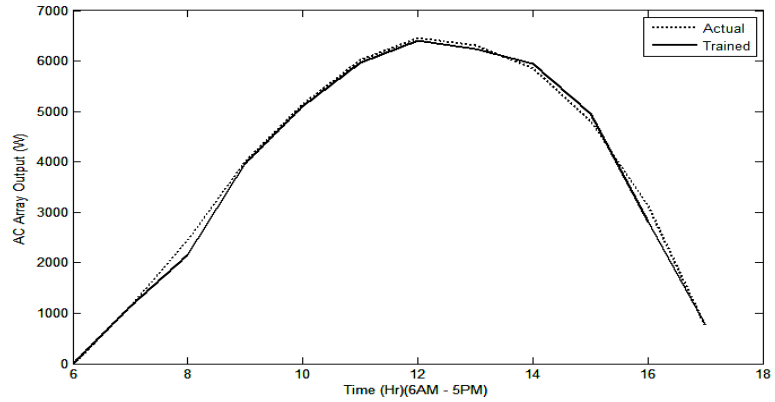

Fig. 14: AC actual and trained output vs time-Winter

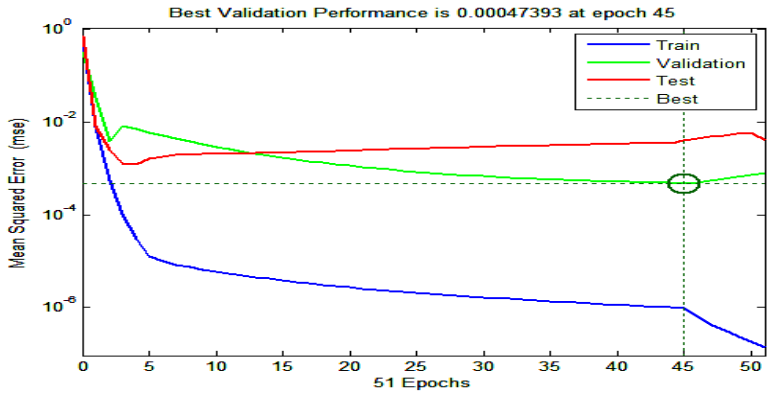

Fig. 15: Performance plot-Summer

Table 3: Power output and eror-Winter

Hours	6AM	7AM	8AM	9AM	10AM	11AM	12PM	1PM	2PM	3PM	4PM	5PM
(W) actual	0	1212.07	2551.49	4157.58	5350.23	6250.56	6711.67	6553.5	6089.05	4997.38	3265.34	796.56
DC(W)trained	13.0	1211.6	2273.4	4150.2	5342.4	6239.0	6698.3	6541.1	6232.0	5215.8	2964.4	754.4
Error	0.002	0.0023	0.041	0.0072	0.0016	0.0011	0.0025	0.0012	0.023	0.033	0.04	0.0061
AC (W) actual	0	1132.02	2438.75	3997.31	5148.42	6013.97	6456.79	6303.97	5857.89	4807.31	3131.54	727.25
AC (W) trained	16.0	1120.7	2161.6	3962.9	5102.4	5961.5	6401.2	6248.2	5946.6	4959.7	2812.8	760.6
Error	0.003	0.019	0.04	0.0011	0.0015	0.0084	0.0018	0.0019	0.022	0.03	0.04	0.006

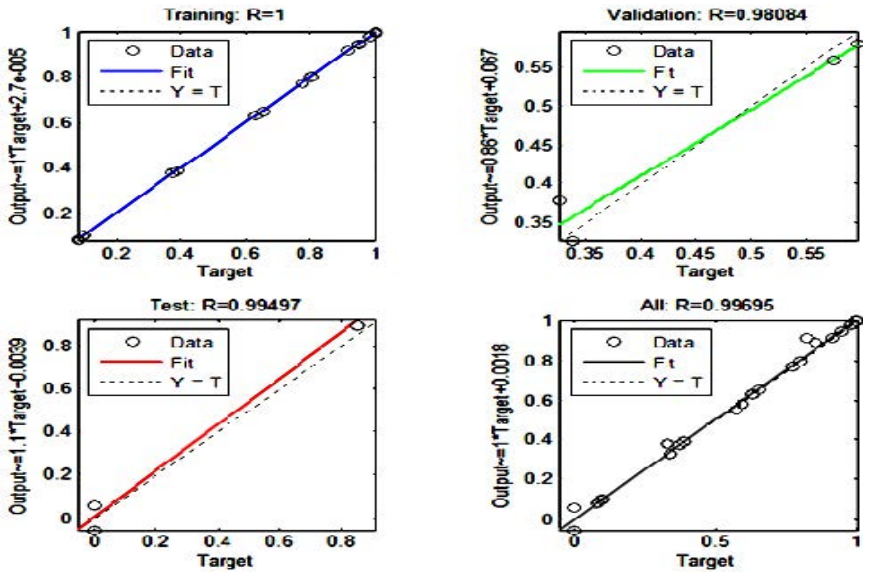

Fig. 16: Training regression plot-summer

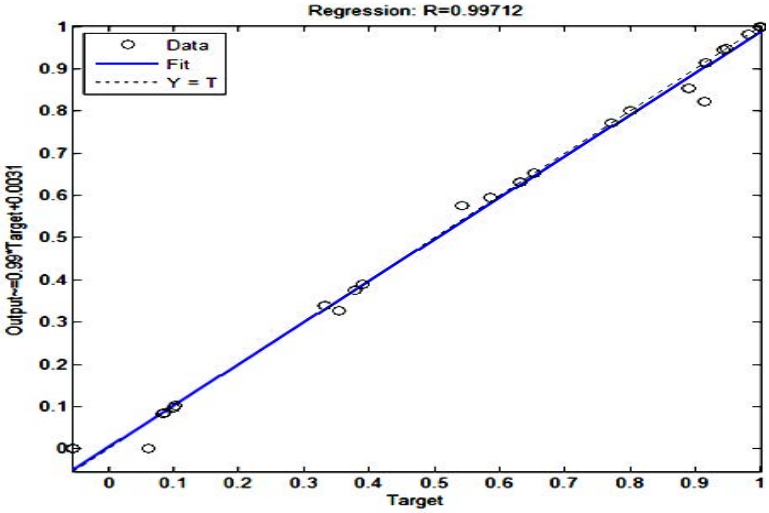

Fig. 17: Testing Regression plot-Summer

Table 4: Power output and eror Summer

Hours	6AM	7AM	8AM	9AM	10AM	11AM	12PM	1PM	2PM	3PM	4PM	5PM
DC (W) Actual	478.54	1035.98	2328.29	3725.81	4848.41	5660.17	5935.0	5834.97	5136.29	4042.01	2601.0	946.73
DC(W)Trained	540.40	1000.20	2218.90	3642.80	4765.10	5494.40	5623.1	5667.00	5004.90	3950.10	2608.8	941.60
Error	0.0200	0.00800	0.00400	0.00200	0.00300	0.01100	0.0300	0.01100	0.0050	0.00600	0.0200	0.0130
AC (W)Actual	422.44	959.830	2221.28	3578.76	4664.36	5446.62	5910.76	5614.43	4941.09	3883.78	2486.2	872.38
AC (W)Trained	534.30	975.000	2151.20	3530.30	4615.50	5315.00	5437.10	5478.00	4846.60	3827.30	2528.8	921.90
Error	0.0240	0.00800	0.00500	0.00100	0.00300	0.01000	0.07200	0.01100	0.00400	0.00400	0.0160	0.0140

how far the data are within the fit at each phase (Fig. 16). From the regression plot (Fig. 17) obtained from testing the network shows how far the data is laying within the fit after testing process. Table 4 represents the forecasted values (trained output) of hourly PV power and measured power (actual output), along with errors for the summer season. Figure 18 and 19 shows the DC, AC actual and trained output, respectively.

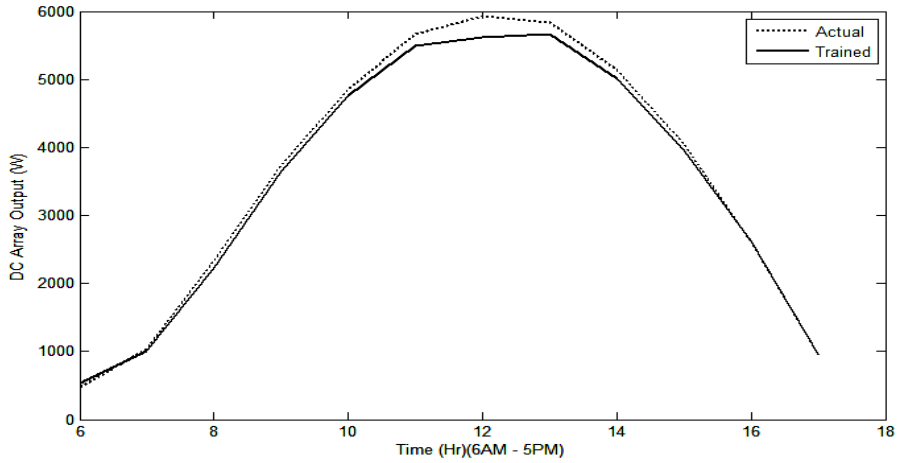

Fig.18: DC Actual and Trained output vs time-Summer

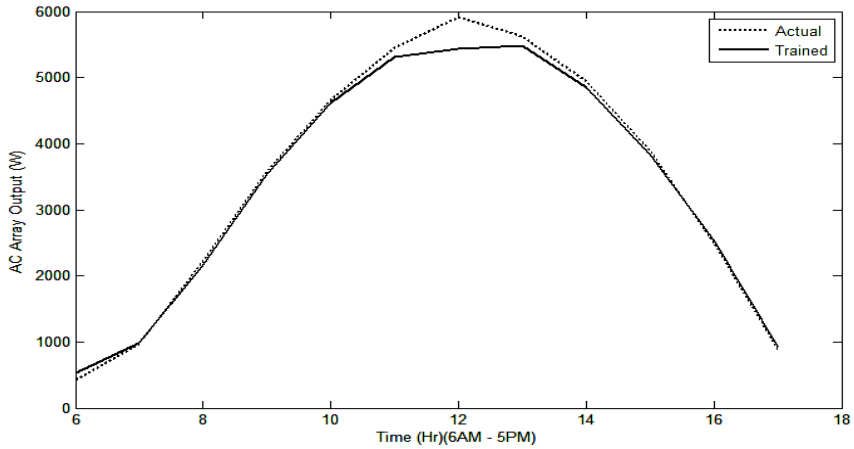

Fig. 19: AC actual and trained output vs time-Summer

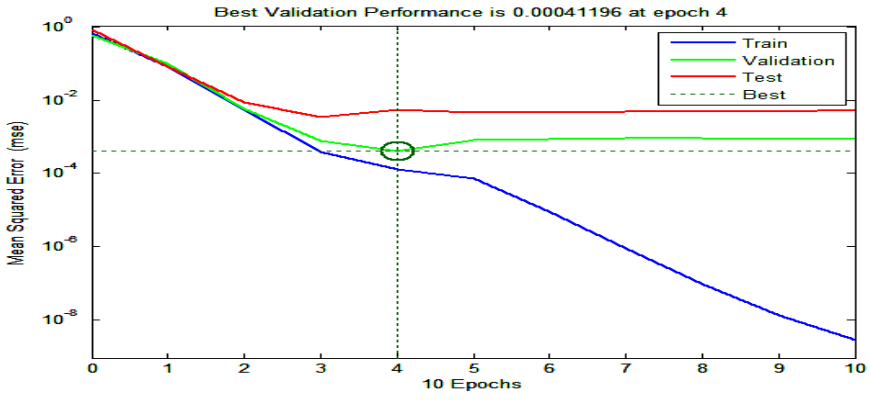

Fig. 20: Performance plot-rainy

Rainy/cloudy season: It is clear from the performance plot (Fig. 20) that the Mean Square Error (MSE) value obtained is nearer to the calculated value, for rainy season. The regression plots obtained after training shows how far the

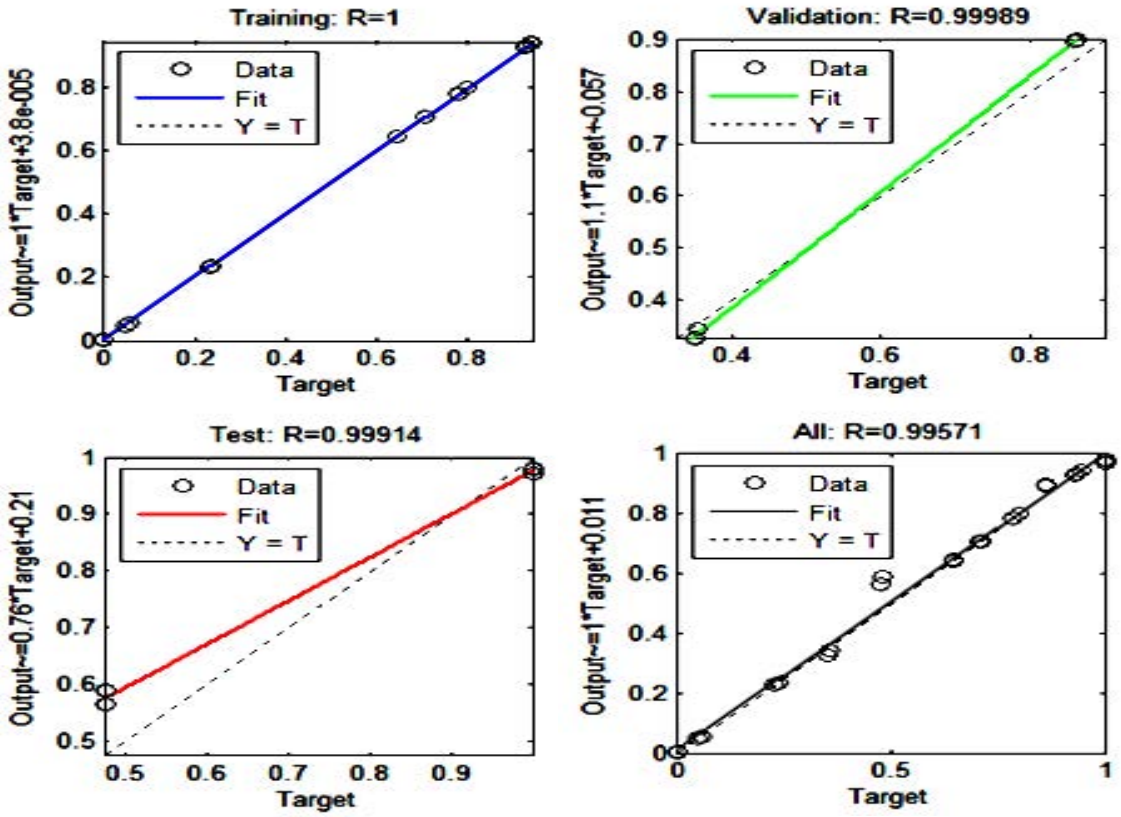

Fig. 21: Training regression plot-rainy

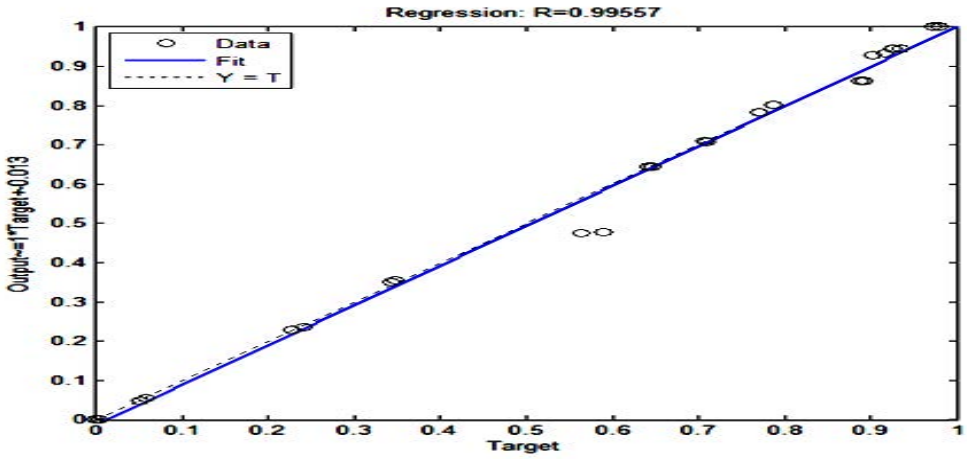

Fig. 22: Testing regression plot-rainy

data are within the fit at each phase (Fig. 21). The regression plot (Fig. 22) obtained from testing the network shows how far the data is laying within the fit after testing process. From the regression plot obtained from testing the network shows how far the data lies within the fit after testing process. The forecasted values (trained output) of hourly PV power and measured power (actual output) for the rainy season are tabulated in Table 5 with their errors. The DC and AC actual and trained output are shown in Fig. 23 and 24, respectively.

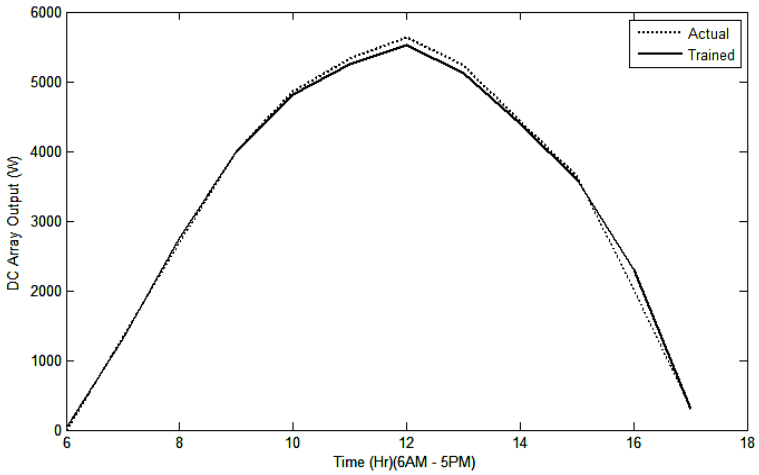

Fig. 23: DC actual and trained output vs time-rainy

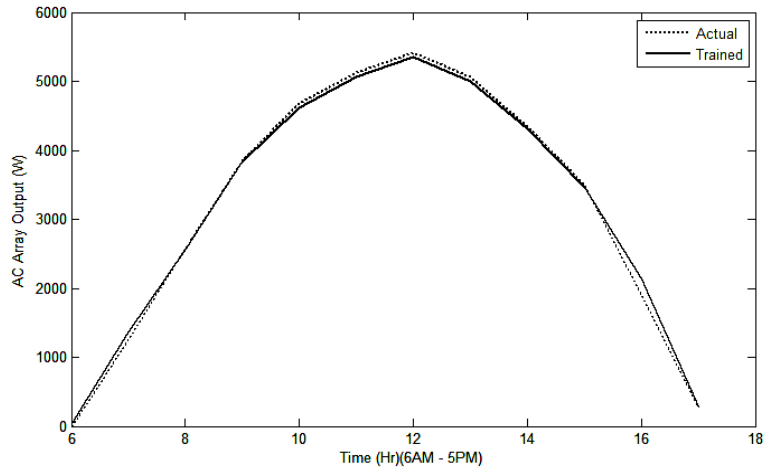

Fig. 24: Actual and trained output vs time-rainy

Table 5: Power output and eror-rainy

Hours	6AM	7AM	8AM	9AM	10AM	11AM	12PM	1PM	2PM	3PM	4PM	5PM
DC (W) actual	00000	1323.56	2691.83	3998.38	4862.55	5333.78	5640.42	5235.69	4422.29	3638.02	2001.06	310.24
sDC(W) trained	39.00	1297.10	2747.10	3988.40	4820.9	5246.10	5526.40	5118.00	4395.10	3593.30	2293.60	297.20
Error	0.007	0.00300	0.01300	0.00300	0.001	0.00800	0.01300	0.01400	0.00800	0.00300	0.05400	0.0010
AC (W) actual	0000	1243.22	2574.80	3841.72	4675.09	5128.04	5423.54	5065.27	4345.24	3491.03	1900.94	259.98
AC (W) trained	3300	1346.60	2546.20	3824.70	4617.2	5065.70	5345.20	5002.30	4310.20	3461.90	2129.20	273.70
Error	0.009	0.0200	0.00300	0.00200	0.0070	0.00700	0.01000	0.00700	0.00300	0.00200	0.04300	0.0020

CONCLUSION

It will be able to obtain much more meteorological data from outer atmosphere with the help of modern remote sensing technology, it is promising to use them for power forecasting of renewable energy generation. In this study, a weather-based classification of data are used for training and testing on BP neural network, for 1-day ahead hourly forecasting of PV power output. Further validations have also been done for a practical roof top solar PV system in Chennai coast india. The proposed method is simple, efficient and accurate for tropical climate region. And better forecasting accuracy might assist power system operators schedule power generation and

spare more reserve capacity for emergencies where large scale rooftop grid connected solar PV penetration is happening in the grid.

REFERENCES

Cao, S., W. Weng, J. Chen, W. Liu and G. Yu *et al.*, 2009. Forecast of solar irradiance using chaos optimization neural networks. Proceedings of the 2009 IEEE Conference on Asia-Pacific Power and Energy Engineering, March 27-31, 2009, IEEE, New York, USA., ISBN: 978-1-4244-2486-3, pp: 1-4.

Capizzi, G., C. Napoli and F. Bonanno, 2012. Innovative second-generation wavelets construction with recurrent neural networks for solar radiation forecasting. IEEE. Trans. Neural Networks Learn. Syst., 23: 1805-1815.

Liu, J., W. Fang, X. Zhang and C. Yang, 2015. An improved photovoltaic power forecasting model with the assistance of aerosol index data. IEEE. Trans. Sustainable Energy, 6: 434-442.

Oudjana, S.H., A. Hellal and I.H. Mahamed, 2012. Short term photovoltaic power generation forecasting using neural network. Proceedings of the 2012 11th International Conference on Environment and Electrical Engineering (EEEIC), May 18-25, 2012, IEEE, New York, USA., ISBN: 978-1-4577-1830-4, pp: 706-711.

Ran, L. and L. Guangmin, 2008. Photovoltaic power generation output forecasting based on support vector machine regression technique. Elect. Power, 41: 74-78.

Shi, J., W.J. Lee, Y. Liu, Y. Yang and P. Wang, 2012. Forecasting power output of photovoltaic systems based on weather classification and support vector machines. IEEE. Trans. Ind. Appl., 48: 1064-1069.

Tanaka, K., K. Uchida, K. Ogimi, T. Goya and A. Yona *et al.*, 2011. Optimal operation by controllable loads based on smart grid topology considering insolation forecasted error. IEEE. Trans. Smart Grid, 2: 438-444.

Wang, S., N. Zhang, Y. Zhao and J. Zhan, 2011. Photovoltaic system power forecasting based on combined grey model and BP neural network. Proceedings of the 2011 International Conference on Electrical and Control Engineering (ICECE), September 16-18, 2011, IEEE, New York, USA., ISBN: 978-1-4244-8162-0, pp: 4623-4626.

Yang, H.T., C.M. Huang, Y.C. Huang and Y.S. Pai, 2014. A weather-based hybrid method for 1-day ahead hourly forecasting of pv power output. IEEE. Trans. Sustainable Energy, 5: 917-926.

Yona, A., T. Senjyu, T. Funabshi and H. Sekine, 2008. Application of neural network to 24-hours-ahead generating power forecasting for PV system. IEEJ. Trans. Power Energy, 128: 33-39.

Yu, T.C. and H.T. Chang, 2011. The forecast of the electrical energy generated by photovoltaic systems using neural network method. Proceedings of the 2011 International Conference on Electric Information and Control Engineering (ICEICE), April 15-17, 2011, IEEE, New York, USA., ISBN: 978-1-4244-8036-4, pp: 2758-2761.